

IAF



IAF - 87 - 211

**Ram Accelerator Direct Launch
System for Space Cargo**

**A.P. Bruckner and A. Hertzberg
Aerospace and Energetics Research Program
University of Washington,
Seattle, WA, USA**

**38th CONGRESS OF THE
INTERNATIONAL ASTRONAUTICAL FEDERATION**

October 10-17, 1987/Brighton, United Kingdom

A. P. Bruckner* and A. Hertzberg†
 Aerospace and Energetics Research Program
 University of Washington, FL-10
 Seattle, WA 98195, U.S.A.

Abstract

The ram accelerator, a chemically propelled mass driver, is presented as a new approach for directly launching acceleration insensitive payloads into low earth orbit. The cargo vehicle resembles the centerbody of a conventional ramjet and travels through a launch tube filled with a premixed gaseous fuel and oxidizer mixture. The tube acts as the outer cowl of the ramjet and the combustion process travels with the vehicle. Two modes of ram accelerator drive are described, which when used in sequence, are capable of accelerating the cargo vehicle to 10 km/sec. The requirements for placing a 2000 kg vehicle with 50% payload fraction into a 400 km orbit, with a minimum of on-board rocket propellant for circularization maneuvers, are examined. It is shown that aerodynamic heating during atmospheric transit results in very little ablation of the nose. Both direct and indirect orbital insertion scenarios are investigated and a three-step maneuver consisting of two burns and aerobraking is found to minimize the on-board propellant mass. A scenario involving a parking orbit below the desired final orbit is suggested as a means to increase the flexibility of the mass launch concept.

Nomenclature

A	frontal area of vehicle
A_t	cross sectional area of launch tube
C_D	drag coefficient of vehicle
C_f	skin friction coefficient
C_p	specific heat at constant pressure
F	thrust
h	heat transfer coefficient
I_{sp}	specific impulse
k	constant
m	mass of vehicle
m_i	initial mass of vehicle
\dot{m}	mass flow rate
M	Mach number
p	static pressure
q	heat load to nose cone
Δq	heat of combustion per unit mass
S	surface area of nose cone
S_t	Stanton number ($h/\rho VC_p$)
t	time
T	static temperature of propellant gas
V	velocity of vehicle
V_e	terminal velocity at "edge" of atmosphere (50 km)
V_i	velocity of vehicle at launch
y	altitude
y_i	altitude of launch
β	atmospheric density decay factor
γ	specific heat ratio
ϵ	heat of vaporization of carbon

* Research Associate Professor of Aeronautics and Astronautics; Member AIAA

† Director; Professor of Aeronautics and Astronautics; Fellow AIAA

θ_i	launch angle
ρ	density of atmosphere
ρ_0	effective sea level density of atmosphere

Subscripts

1	conditions in tube upstream of vehicle
5	conditions at aft end of vehicle in superdetonative mode
6	conditions at thermal choking point in subsonic combustion mode

I. Introduction

One of the key problems in developing a permanent large-scale space infrastructure designed for space manufacturing, or for the full exploration and colonization of our solar system, is the relatively high cost of launch systems capable of carrying the raw materials necessary to construct the large space systems required. Much of this material, such as the components of large space structures, the various raw materials of space manufacturing, and hydrogen, oxygen, and other supply elements are capable of withstanding high launching stress. This stress insensitivity has attracted the attention of scientists and engineers over the years, and various mass launchers to carry out the function of direct launch have been proposed.¹⁻¹⁴ These have ranged from hypervelocity guns to various electrical accelerators.³⁻¹³ The relatively low efficiency of the former and the formidable problem of dealing with the management of the large instantaneous electric power loads in the latter, have proved to be serious barriers to their implementation.

At the University of Washington a ramjet-in-tube concept called the "ram accelerator" has been developed for efficiently accelerating relatively large masses (up to several metric tons) from velocities of 0.7 km/sec up to 12 km/sec using chemical energy.¹⁵⁻²⁰ The propulsion cycle of the ram accelerator is similar to the aero-thermodynamic cycle which generates the thrust in a conventional airbreathing ramjet; however, the device is operated in a different manner. The vehicle, which resembles the centerbody of a conventional ramjet, travels through a tube filled with a premixed combustible gas mixture of fuel and oxidizer (see Figs. 1 and 2). The tube acts as the outer cowl of the ramjet and the energy release process travels with the vehicle. The acceleration can be maintained at a nearly constant level over the entire velocity range of operation. The concept is scalable for vehicle masses ranging from grams to thousands of kilograms and has the potential for a number of applications of interest, such as hypervelocity impact studies and direct launch to orbit of acceleration insensitive payloads.

Several modes of ram accelerator operation have been investigated by the authors; these modes differ primarily in the method of chemical heat release and the operational velocity range.¹⁵⁻²⁰ Two modes relevant to the direct launch concept are illustrated in Figs. 1 and 2. The first of these (Fig. 1) uses thermally choked subsonic combustion behind the vehicle and is suitable for the velocity range of 0.7-3 km/sec.* The second (Fig. 2) uses the heat release in the oblique detonation wave generated by the reflected bow shock to produce the forward thrust. In principle, this mode of propulsion is capable of efficient acceleration in the range of 3-12 km/sec. Laboratory scale experiments on the thermally choked subsonic combustion mode have been carried out at the University of Washington. Velocities of ~2 km/sec and accelerations up to 20,000 g have been achieved with a 60 gm projectile in a 38 mm bore tube, and proof of principle of the ram accelerator concept has been established. The results have shown a remarkably close agreement between predicted and measured performance^{15,16}.

The systems definition for direct launch lends itself to a number of possible operational configurations. A launch system capable of delivering a 2000 kg vehicle with at least a 50% payload fraction into low earth orbit (LEO) has been selected for the purposes of the present study.²⁰ The peak permissible acceleration has been limited to 1500 g as a compromise between reducing vehicle structural mass and limiting the length of the launch tube. The following key issues are examined here: 1) the vehicle must be accelerated to a velocity of the order of the orbital velocity or higher; 2) the vehicle must survive the stresses resulting from the launch acceleration; 3) the vehicle must survive atmospheric transit and maintain its integrity with good thermal protection for the cargo; 4) the necessary orbital maneuvers must be accomplished with a minimum amount of on-board rocket propellant. To date, only the aspects of technical feasibility have been addressed. The possible economic advantages of this concept could only be approached indirectly. For example, in order to reduce costs, exotic technology was avoided, cheap propellants were selected, and the potential reusability of the vehicle was explored.

II. Analysis of Ram Accelerator Drive Modes

The ram accelerator drive modes have been modeled using a one-dimensional, quasi-steady, inviscid approach.^{15,16} More recently, a 2-D axisymmetric inviscid CFD code has been used in the analysis of the oblique detonation drive mode.¹⁸ Here we present only a brief summary of the relevant features of the 1-D models as they apply to the two propulsive modes considered for the direct space launch scheme.

Subsonic Combustion Mode

In the subsonic combustion ram accelerator mode (Fig. 1) the cone angle of the nose is chosen such that the oblique shock system in the diffuser

* The initial acceleration to the 0.7 km/sec entrance velocity of the ram accelerator is accomplished by means of conventional gas gun technology.

does not initiate combustion at any velocity within the operational range of this mode. A normal shock too weak to ignite the gas mixture is located downstream of the diffuser throat. This shock renders the flow subsonic with respect to the vehicle. The recirculation zone at the base of the vehicle acts as a flameholding dump combustor. The normal shock is stabilized on the vehicle because the heat release of combustion chokes the flow at the full tube area behind the vehicle. The resulting pressure distribution on the vehicle produces forward thrust.

This ram accelerator mode is amenable to a particularly straightforward approach which results in a closed form analytical solution for the thrust on the vehicle. Applying the momentum conservation equation to the control volume defined in Fig. 1 by stations 1 and 6 and the launch tube, yields the equation for the thrust:

$$F = (p_1 A_t + \dot{m}_1 u_1) - (p_6 A_t + \dot{m}_6 u_6) \quad (1)$$

Combining Eq. 1 with the equations of conservation of mass and energy, and noting that $M_6 = 1$, i.e., the flow leaving the control volume is thermally choked, yields the following relation for the non-dimensional thrust parameter, $F/p_1 A_t$, on the vehicle¹⁵:

$$\frac{F}{p_1 A_t} = \frac{\gamma_1 M_1}{\gamma_6} \left\{ 2 \left(\frac{\gamma_6^2 - 1}{\gamma_1 - 1} \right) \left[1 + \frac{\gamma_1 - 1}{2} M_1^2 + \frac{\Delta q}{C_{p1} T_1} \right] \right\}^{1/2} - (1 + \gamma_1 M_1^2) \quad (2)$$

The subscripts 1 and 6 denote the upstream and downstream boundaries of the control volume shown in Fig. 1.

The thrust, and thus the acceleration of the vehicle, is directly proportional to the tube fill pressure. The in-tube aerodynamic friction is so small compared to the thrust that it can be neglected.¹⁵

As the projectile accelerates, the thrust decreases, reaching zero at a flight Mach number which corresponds to that of a one-dimensional Chapman-Jouguet (C-J) detonation wave propagating in the same gas mixture.¹⁵ This is the limiting velocity for the thermally choked subsonic combustion mode of propulsion. In the laboratory the authors have attained projectile velocities of ~85% of the C-J velocity in propellant mixtures of methane and oxygen, with nitrogen, carbon dioxide or helium as diluents.¹⁶ Thus, by using fuel-rich hydrogen-oxygen propellant mixtures, velocities of ~3000 m/sec should be attainable using the thermally choked subsonic combustion drive mode. Accordingly, for the purposes of the present paper, this velocity has been chosen for the transition to the oblique detonation mode.

Optimum performance is obtained by keeping the vehicle Mach number within a narrow range close to that corresponding to the peak thrust. This can be accomplished by filling the launch tube with a graded propellant mixture whose acoustic speed increases in the direction of vehicle travel or by dividing the launch tube into several segments filled with different propellant mix-

tures, and constraining the vehicle to operate over a limited Mach number range in each segment.

Figure 3 shows plots of the non-dimensional thrust parameter (Eq. 1) as a function of vehicle velocity for three representative propellant mixtures which could be used to accelerate the vehicle from a velocity of 0.7 km/sec to 3 km/sec. The dotted lines show appropriate transitions between the different mixtures.* Based on this example, the propellant fill pressure necessary to accelerate a 2000 kg, 0.76 m diameter vehicle in a 1.0 m I.D. launch tube at < 1500 g is 50 atm. With this initial pressure, a peak cycle pressure of 1450 atm is reached at the end of the third mixture. The length of launch tube required to reach 3 km/sec with the acceleration profile of Fig. 3 is 354 m.

Oblique Detonation Mode (Superdetonative)

In the oblique detonation concept (Fig. 2), the nose cone angle, vehicle velocity and acoustic speed of the combustible gas mixture are selected such that the initial conical shock does not initiate combustion but the reflected shock from the tube wall does. In operation, the reflected shock becomes an oblique detonation wave, which may be either C-J or overdriven. The vehicle geometry and tube to vehicle diameter ratio are chosen so that the reflected detonation wave strikes the vehicle just aft of the shoulder. The flow remains supersonic throughout. Because the detonation drive mode operates at vehicle velocities which exceed the local C-J detonation speed, it will henceforth be referred to as the "superdetonative" mode.

Although the general thrust equation for the superdetonative mode is similar to Eq. 1, with the subscript 6 replaced by 5 (see Fig. 2), no simple closed-form solution exists and the thrust must be determined numerically.¹⁷ The incident oblique shock is calculated by applying the equations of continuity, momentum (in two dimensions) and energy across the shock. The reflected oblique detonation wave is computed in a similar manner with a heat addition term included in the energy equation. The conditions at station 4 are determined by applying the conservation equations between this station and the station just downstream of the detonation wave. The nozzle flow from station 4 to station 5 is treated isentropically. An ideal gas equation of state is assumed with one set of values of γ and molecular weight before combustion and a second set after combustion.

The temperature after the initial compression by the bow shock, but before combustion, is limited to a maximum of 900°K. Cycle solutions with higher post compression temperatures are assumed to be at risk for combustion and are rejected as practical cycle solutions. In addition, valid solutions are required to have temperatures behind the reflected shock (without combustion) exceeding 1100°K to ensure initiation of the detonation.

*Transition between different mixtures has been experimentally demonstrated by the authors.¹⁶

Figure 4 shows curves of the non-dimensional thrust parameter, $F/p_1 A_t$, versus velocity for the superdetonative mode. The half-angle of the nose was assumed to be 12.5°. This value is necessary to produce sufficient compression across the bow shock to ensure that the reflected wave is a detonation even at the low velocity limit (3.0 km/sec) of this mode of propulsion. Each curve represents a different propellant mixture identified in Fig. 4. These were chosen to have overlapping regimes of operation to span the velocity range of 3 to 10 km/sec. The dotted lines indicate appropriate velocities at which to make transitions between the mixtures to maximize the overall average thrust. For a tube fill pressure of 50 atm, a peak cycle pressure of 4450 atm is reached in mixture #2.

Mode Transition

The vehicle geometries required for the two modes of propulsion discussed above are sufficiently similar that a single configuration can be designed to operate using both modes in sequence to attain the desired velocity. The transition from the subsonic combustion mode to the superdetonative mode is effected by an abrupt change of propellant mixture in the accelerator tube at the location where the necessary transition velocity of 3 km/sec is achieved. In the example presented here the transition occurs from a mixture of $4H_2 + O_2$ to one of $2H_2 + O_2 + 2N_2 + 3A_r$. At transition the Mach number suddenly increases from 4.5 to 8.3 because the second mixture has a much lower speed of sound. The oblique detonation wave is automatically established on the vehicle. A thin diaphragm can be used to separate the gas mixtures.

In-Tube Velocity Profile

The velocity profile of the in-tube flight of the vehicle is determined by integrating the equation of motion of the vehicle. The results are shown in Fig. 5 for a tube fill pressure of 50 atm. The overall length of launch tube required to accelerate the 2000 kg vehicle from a standing start varies from 1.75 km at 7 km/sec to 4.0 km at 10 km/sec.

III. Vehicle and Launch Tube Configuration

Vehicle

In carrying out the vehicle design studies, preliminary configurations of an integrated vehicle were developed. The configuration used in the current study is shown in Fig. 6. The vehicle diameter is 0.76 m and its overall length is 6.0m. Behind the ablative nose-cone are located the main orbital maneuvering solid propellant rocket and the hydrazine monopropellant rocket used for final orbital maneuvers. Both rocket units have four symmetrical nozzles pointing forward. These nozzles are initially shielded by expendable ablating covers. By placing the on-board rocket units in the forward portion of the vehicle the volumetric utilization of the vehicle for the payload is maximized. The structural aspects of the portion of the vehicle forward of the payload section are currently being considered by the authors in ongoing studies and will be reported in a future publication. The payload section design is discussed briefly in the following paragraphs.

The structural design of the payload vessel in the ram accelerator mass launcher represents a key to the overall success of the concept. The goal is to design the payload vessel to resist all loads imposed by the ram accelerator while minimizing the mass necessary to do so. A suitable structural design capable of carrying a 1000 kg payload of water was investigated. The optimum configuration was determined to be a vessel whose shape is integrated directly into the vehicle's body. The material chosen was graphite epoxy because of its high strength and light weight.

The loads experienced by the payload vessel while the vehicle is in the launch tube of the ram accelerator are far greater than any loads experienced anywhere else during the mission. Therefore, if the vessel can withstand these loads, survival of the payload will be assured. The outer configuration of the vehicle must satisfy the geometrical design for the aft end imposed by the gasdynamic cycle considerations. This can be best accomplished by incorporating the vessel into the rear end geometry of the vehicle as shown in Fig. 6. The load generated by the structural mass of the vehicle ahead of the cargo vessel (i.e. nose cone, rocket systems, etc.) is assumed to be transmitted directly to the cylindrical walls of the vessel.

Due to the hydrostatic loading of the liquid payload, a hoop stress is developed within the structure which increases linearly towards the rear of the structure. The cylinder also experiences a compressive loading from the acceleration of the mass of the cylinder wall and the mass of the forward portion of the vehicle, and a compressive hoop stress from the external cycle pressure. With the computation of the hoop and longitudinal stress under the given loading conditions, the parameters of design are optimized by choice of the ply layup and lamination thickness of the composite material. The criterion for failure is the maximum strength criterion applied to the first ply failure mode of the composite material.

The number of the ply layups within the sub-laminate was chosen in such a way as to maximize the strength to mass ratio. The total mass of the cargo carrying portion of the vehicle was determined to be ~ 185 kg.²⁰ It is estimated that the remaining structural mass of the forward portion of the vehicle, including the ablative nose cone, will not exceed this value.

Launch Tube and Initial Accelerator

The launch tube presents interesting design problems of its own. For the point design discussed here the tube will have a length between 1.75 and 4 km, depending on the selected launch velocity. The tube material and wall thickness must be such as to withstand the peak pressures imposed by the propulsive cycles. In each mode the heat and pressure pulses travel with the vehicle, distributing the heat over the entire length of the launch tube. Consequently, the temperature rise of the tube is very small and very little tube wear is expected. Indeed, after several hundred shots the authors have yet to detect any tube wear in their experimental facility.

For present purposes it is conservatively assumed that the launch tube must contain the peak cycle pressure in static loading and that the tube is manufactured from high strength steel alloy (200,000 psi yield). The peak pressure in both the initial gas gun and the subsonic combustion mode is ~ 1500 atm, while in the superdetonative mode it is 4450 atm. The respective tube I.D.'s are 0.76, 1.0 and 0.85 m. Including a safety factor of 2, the required wall thicknesses of the three tube sections are respectively 9.6 cm, 12.6 cm and 50 cm. To accelerate a 2000 kg vehicle to 9 km/sec, for example, would require a launch tube 3.15 km long, which would have a mass of ~ 48,500 metric tons, about the same as a large ocean liner. The technology for fabricating and laying such a tube up the side of a mountain with the appropriate average slope is similar to that developed for laying pipelines and should not present undue difficulties.

In order to contain the 50 atm propellant gas mixtures in the ram accelerator tube prior to launch, some form of closure must be used both at the entrance and exit of the launch tube. These closures could be thin, petaling, Kevlar diaphragms or fast-acting mechanical shutters. The exit closure could be explosively removed just before the vehicle arrived, as there would then no longer be any risk of pre-igniting the combustible gas fill. A diaphragm is also required at the point of transition between the thermally choked subsonic combustion mode and the superdetonative mode. This diaphragm, however, can be very thin since it does not have to support a pressure differential. On either side of this diaphragm the propellant composition would be appropriately graded to maximize the performance of the ram accelerator propulsive modes over their operational velocity ranges. The gases would be delivered to the launch tube at suitable intervals along its length by turbine-driven pumps.

The design of the initial accelerator is also straightforward. Its requirement is to accelerate the vehicle from a standing start to the 700 m/sec necessary for injection into the ram accelerator tube. In the laboratory the authors have used a simple, single-stage helium gas gun.^{15,16} For the direct launch system it is proposed to use a combustion-driven gas gun. Such devices are technologically well developed for smaller calibers²¹, however, there does not appear to be any serious impediment to scaling up the concept to accommodate a ram accelerator vehicle. For example, during World War II the Germans used two artillery pieces with an 88 cm bore, which is larger than the diameter of the ram accelerator vehicle considered here. Assuming a modest piezometric ratio of ~ 1.8 and a peak acceleration of 1500 g, the length of the initial launcher would be 30 m.

IV. Atmospheric Transit and Aerodynamic Heating

Once the vehicle exits the launch tube it performs the atmospheric transit phase of its journey. At launch velocities of 7-10 km/sec the vehicle undergoes severe aerodynamic heating which necessitates some type of thermal protection to preserve its integrity. The emphasis in this

paper is on an ablative heat shield, although a transpiration cooled nose-cone has also been considered.²⁰ For the ablative case it is necessary to provide the required thermal protection with as low an ablator mass as possible, so that the vehicle can carry as much payload as possible.

The vehicle has a nose-cone half-angle of 12.5°, an initial mass of 2000 kg, a diameter of 0.76 m, and a carbon-carbon composite ablating material nose-cone construction. The nose-cone half-angle is set by the propulsive requirements, as noted earlier. This results in an initial hypersonic drag coefficient of 0.09. Launch velocities in the range of 7-10 km/sec, launch angles of 10°-35° and launch altitudes of 0-4.5 km have been considered. At high launch altitudes the lower air density will result in less drag and in less aerodynamic heating. Thus, higher launch altitudes reduce the thermal protection requirements and the amount of on-board rocket propellant. The maximum launch altitude of 4.5 km was chosen arbitrarily, but it is an altitude that can be reasonably attained in many parts of the world at relatively low latitudes. The launch velocities of 7-10 km/sec and angles of 10°-35° encompass a representative range of potential launch scenarios for achieving LEO.

In-Tube Heating

Although the problem of in-tube heating at velocities above about 7 km/sec is not trivial and requires further study, it is not considered in detail in this paper. In-tube heating is to a certain extent alleviated since the composition of the propellant mixture inside the launch tube is varied such that its acoustic velocity increases toward the muzzle, thus maintaining the vehicle Mach number below ~ 12, even at 10 km/sec. This limits the stagnation temperature, and thus the heat transfer. If the mixture composition is also varied radially and hydrogen is used at the core, the surface temperature at the nose tip will be low enough that sublimation of the carbon-carbon composite will not occur over the range of launch velocities contemplated.²⁰

Ablation and Shape Change During Atmospheric Transit

When the vehicle enters the atmosphere, the nose-cone is subjected to a much higher stagnation temperature than in the launch tube because of the sudden increase in Mach number, and begins to ablate. The ablation process is assumed to be axisymmetric and the surface is assumed to remain smooth.* The recession of the nose cone, however, is not uniform because the heat transfer at the tip, i.e. the stagnation point, is much higher than at the side wall of the cone. Since the angle of a cone remains essentially constant during ablation²², the recession of the surface has been modeled by a cone with a spherical cap, where the radius of the cap increases with mass loss. This approximates the effect of blunting that will actually occur.

The velocity range of concern is sufficiently low that the heating is convective only.²³

* These assumptions are reasonable because the total ablated mass turns out to be very small.

Because the Reynolds number is so high (on the order of 10⁹) the flow is turbulent. Any dissociation that may occur due to the jump conditions across the shock has been neglected in the analysis. The heat transfer that is calculated in this manner is a conservative, i.e. high, estimate.

The equation of motion for a vehicle traversing the atmosphere is

$$m \frac{dV}{dt} = -\frac{1}{2} C_D \rho V^2 A \quad (3)$$

where gravity is neglected because the drag term is much larger than the gravitational force during atmospheric transit. The heat input to the vehicle is²³

$$\frac{dq}{dt} = \frac{1}{2} St \rho V^3 S \quad (4)$$

Assuming an isothermal atmosphere, $\rho = \rho_0 e^{-\beta y}$, where $\rho_0 = 1.752 \text{ kg/m}^3$ and $\beta = 1.49 \times 10^{-4} \text{ m}^{-1}$,²⁴ and using Reynold's analogy, $St = C_f/2$, it can be shown that the mass loss as a function of altitude from launch is given by²⁰

$$\frac{dm}{dy} = -\frac{C_f V^2 S \rho_0 e^{-\beta y}}{4(\xi + kV^2) \sin \theta_f} \quad \rho = \rho_0 e^{-\beta y} \quad (5)$$

where V is obtained from

$$\frac{dV}{dy} = -\frac{C_D A \rho_0 V e^{-\beta y}}{2m \sin \theta_f} \quad (6)$$

In Eq. 5 the quantity kV^2 in the denominator represents the effect that ablation has in reducing heat transfer through the boundary layer; k is a constant whose value is 0.1 for turbulent flow and 0.3 for laminar flow. The mean value of C_f was computed using the method of Van Driest²⁵, assuming a wall temperature of 4000 K. A value of $C_f = 0.00056$ was determined for the case of no ablation but with heat transfer. The heat of vaporization of carbon was taken to be that for C_3 , $2.28 \times 10^7 \text{ J/kg}$.²⁶ C_D was computed from the pressure drag for a three dimensional body of revolution²⁷, with the effect of nose blunting included.

For a given change in altitude, a mass loss was found. This mass loss was subtracted from the body and a new shape was found using the ablation model discussed earlier. The C_D of the new shape was determined and the change in velocity calculated. The rate of mass loss by ablation was found to become negligible at altitudes above ~ 30 km.

The total mass lost by ablation of the nose was found to be very small at any of the launch velocities and angles considered. Figure 7 shows representative results as a function of initial velocity and launch altitude for an initial angle of 20°. Even at 10 km/sec initial velocity the mass loss is only 23 kg, about 1% of the vehicle mass. The ram accelerator concept can thus launch a payload to orbit with good thermal protection and no damage to the payload. The ratio of the terminal velocity of the vehicle at 50 km to the initial velocity of the vehicle, vs. launch angle and initial altitude is shown in Fig. 8. The advantage of launching at the highest possible

altitude is clearly evident. The value of C_D changes very little because the low amount of ablation does not blunt the nose very much. Accordingly, for the purposes of the trajectory computations an average value of $C_D = 0.1$ was assumed.

Transpiration Cooling

Transpiration cooling has also been considered as an alternative thermal protection scheme.²⁰ This method offers the possibility of complete reusability of the vehicle. Previous studies have shown that a low molecular weight coolant maximizes the reduction of the skin-friction coefficient.²⁸ Ammonia, NH_3 , has a relatively low molecular weight, especially after dissociation to its elements, and can be stored as a liquid. To maintain a surface temperature of 1800° K, the mass of coolant needed for the proposed vehicle is ~ 200 kg, which is a significant fraction of total vehicle mass. Even if much higher wall temperatures were tolerable the mass of coolant required would greatly exceed the mass lost by an ablative nose. Coupled with the greatly increased complexity of this method of thermal protection, this fact eliminates transpiration cooling as an acceptable approach for any direct launch scheme.

V. Orbital Mechanics

A major influence in the design and feasibility of any direct launch scheme is the payload mass fraction the vehicle can carry. To maximize the payload, the propellant needed for orbital maneuvers must be minimized. This can be accomplished by selecting the orbital path that requires the least amount of propellant burn to attain the desired orbit, e.g. that of the space station, in an acceptable time frame.

The major problem with launching directly to a space station or orbiting platform in a non-equatorial orbit is that the time of launch from earth is limited to specific time intervals. The method itself is sound, but it limits the rate at which vehicles can be launched from earth and received at the space station, thus increasing the launch costs. Any solution to the orbital transfer problem must maximize the rate at which vehicles can be launched from earth and delivered to the space station, as well as minimize the amount of time and effort required of the ram accelerator and space station crews. The solution is to make use of a parking orbit below the space station orbit.

Parking Orbit

The parking orbit has the same inclination as the space station orbit but a different altitude. Its purpose is to hold a large number of vehicles, which have been launched previously from the ram accelerator, for future use by the space station. Such an orbit allows vehicles to be launched at more frequent intervals than a direct launch to the space station orbit itself, and enables the space station crew to extract the vehicles from the parking orbit as required. The altitude of the parking orbit can be higher or lower than that of the space station, but the lower one is preferable because it has lower energy requirements and

it minimizes the time involved in the orbital transfer process. A safe operating separation of 50 km from the space station has been selected. For the special case of equatorial orbits the vehicles can be launched into the parking orbit as frequently as desired because as the earth turns the launch point always remains in the same plane as the orbit.

Circularization Maneuvers

The analysis of the orbital maneuvers necessary to bring an object from the "edge" of the atmosphere (defined as 50 km altitude for present purposes) to a desired circular parking orbit requires that certain parameters be known at certain points in the trajectory. Given the initial mass, speed, position, and launch angle of the vehicle, and the specific impulse of onboard propellant, the necessary maneuvers and propellant burns can be calculated.

Conventional wisdom for minimizing the amount of propellant needed to circularize the orbit of an impulsively launched vehicle is to launch it in such a manner that its ballistic apogee is at the altitude of the desired circular orbit,⁵ as shown in Fig. 9a. The propellant mass ratio required for such a maneuver is shown by the dashed curves in Fig. 10, as a function of initial velocity and launch altitude for the case of a parking orbit at 350 km and a final orbit at 400 km. The orbits are assumed to be equatorial. The first burn to circularize at 350 km was assumed to have an Isp of 300, while the final burns to attain the 400 km orbit were assumed to have Isp's of 245. For a given orbit, launch velocity, and launch altitude there is a unique launch angle which places the apogee at the desired altitude. As the initial velocity is increased, the launch angle must be reduced, thus incurring an increasing penalty in aerodynamic drag. For example, for a sea level launch the launch angle decreases from 22.5° at 7 km/sec to 14.8° at 10 km/sec. At 4.5 km initial altitude the corresponding figures are 17.4° at 7 km/sec and 9.7° at 10 km/sec.

Multi-Step Maneuver: A more economical maneuver investigated by the authors consists of two burns with an atmospheric braking maneuver between the two burns, as shown in Fig. 9b. The vehicle is launched at a higher initial angle, so that its ballistic apogee is above the desired parking orbit. At the apogee, a burn is performed which raises the perigee enough so that the vehicle's path misses the earth's surface but remains in the atmosphere, which in turn brakes the vehicle and lowers the apogee. A second burn is then made at the new apogee to circularize the parking orbit. For the range of launch velocities and angles considered, the perigee altitude lies approximately in the range of 30-50 km for the aerobrake maneuver. The intrinsic drag of the vehicle is sufficient to perform the necessary aerobraking ΔV for a broad range of launch parameters. Thus no special aerodynamic devices are required to enhance the drag. Because the necessary ΔV 's are generally under 1000 m/sec, the aerodynamic heating during the aerobrake maneuver is not severe.

The amount of on-board rocket propellant needed to maneuver the ram accelerator vehicle to the desired orbit using this approach is directly dependent upon four major variables: the initial

velocity of the vehicle, the launch angle, the launch altitude and the specific impulse of the on-board propellant. Because the initial burn of the orbital maneuvers requires the most propellant, optimizing the initial launch conditions is critical to reducing the overall amount of propellant necessary to complete the orbital maneuvers. In the absence of an atmosphere, the optimum launch angle for any initial velocity would be 0° (i.e., tangent to the earth's surface) because the trajectory would then most closely approximate a Hohmann transfer. However, because of the presence of the atmosphere, lowering the launch angle increases the atmospheric drag on the vehicle and thus decreases the atmospheric exit velocity. An optimal launch angle can be determined for any given initial velocity and altitude.

The variation of total propellant mass fraction with launch angle for various initial velocities at launch altitudes of 1.5 and 4.5 km is shown in Fig. 11, for an equatorial launch. This mass fraction includes the propellant required for the final transfer to a space station orbit at 400 km. As expected, the propellant mass fraction required for maneuvers decreases with increasing initial velocity and increasing launch altitude. The optimum launch angle is in the range of 27° - 17° for velocities of 7-10 km/sec. The minimum possible launch angle for a given combination of launch altitude and velocity is that for which the ballistic apogee is just at the parking orbit's altitude. Changes in the initial velocity have a sizable effect on the necessary propellant burn. The reason for this phenomenon is that higher initial velocities result in higher orbital apogee velocities, and a larger orbital apogee velocity results in lower propellant burns to produce the change in velocity required to obtain the desired perigee altitude for aerobraking.

The solid curves in Fig. 10 show the dependence of the propellant mass fraction on the initial launch velocity for several launch altitudes. For each combination of velocity and altitude the optimum launch angle was used. It can readily be seen that the multiple-burn-with-aerobrake maneuver requires less propellant than the direct insertion maneuver, especially at the higher launch velocities. The reason for this greater propellant economy is that the multiple maneuver scheme optimizes at a higher launch angle than the direct insertion maneuver and thus the vehicle exits the atmosphere at a higher velocity.

To conduct a Hohmann transfer between the parking and final orbits, the vehicle and the space station must be in the proper initial positions if a rendezvous is to occur.²⁹ The rate of transfer of vehicles to the space station is determined by the time it takes the space station and the vehicle to make the necessary initial relative angle. Table 1 lists the time to conjunction as a function of the number of vehicles in the parking orbit. If the rate of transfer of vehicles to a space station in equatorial orbit is assumed equal to the expected maximum rate-of-fire of the ram accelerator (approximately every 2 hrs) the optimum steady state number of vehicles in the parking orbit is 69. Assuming a payload fraction of 50%, this rate of fire would permit delivering 12,000 kg of materials and supplies daily to a space station in equatorial orbit.

TABLE 1

Number of Vehicles	Angular Spacing	Time to Reach Conjunction
1	360°	138.1 hrs
5	72°	27.62 hrs
10	36°	13.8 hrs
25	14.4°	5.52 hrs
50	7.2°	2.76 hrs
69	5.22°	2.0 hrs
100	3.6°	1.38 hrs

Disposition of Spent Vehicles

The disposition of the ram accelerator vehicles, once they have been intercepted and unloaded by the space station crew, presents several possible options: 1) discard them in orbit, 2) disassemble them and use the payload vessels to store materials at the space station, 3) use them as sources of material for space structures or other uses, 4) use tether techniques to send clusters of them back to earth on re-entry trajectories for refurbishment and re-use. Clearly, option 1 must be ruled out because of the severe orbital clutter that would result. Options 2 and 3 are more desirable but place additional design constraints on the vehicles to optimize their adaptability to other uses. Option 4 would require that the ablative shield be designed to also survive atmospheric re-entry, which would place a much more severe heat load on the vehicle than the initial upward leg of the journey. In addition, the vehicle would have to be equipped with drag brakes and parachutes for the final phase of recovery before splashdown. These requirements would result in a decrease of the payload fraction, and an increase in the complexity of the control system. In addition, recovery and refurbishment operations would have to be implemented. Which of the options turns out to be the most desirable will depend on their relative impacts on overall launch costs. This issue is currently under study.

VI. Conclusions

The ram accelerator offers a promising new approach for the direct launch of acceleration insensitive cargo to low earth orbit. Using the controlled release of chemical energy in a propulsive cycle similar to that of a conventional ramjet, the device is capable of accelerating cargo vehicles of up to several metric tons to velocities as high as 10 km/sec at a nearly constant acceleration. Payload mass fractions of 50% or better are achievable. Aerodynamic heating during atmospheric transit of a 2000 kg vehicle results in very little ablation at any of the launch velocities considered. The most economical orbital insertion scheme consists of three Hohmann transfers involving a burn at first apogee, followed by an atmospheric braking maneuver at first perigee, and a second burn for circularization at the second apogee. By placing the vehicles in a parking orbit below the desired final orbit, the launch and interception events are made independent, thus increasing the flexibility of the mass launch concept.

Acknowledgements

This work was supported in part by the NASA/USRA University Advanced Design Program and by NASA Grant NAG-1-746. The authors are indebted to their students Peter Kaloupis, Kevin Kellegrew, Supriya Ghosh, John Diamond, Scott McKeel, William Vlases, Quentin Dierks, David Evans, Karl Heilborn Jr. and Yung Ford, for performing the preliminary system design which formed the basis for this paper. Many thanks are also due to David W. Bogdanoff for his many useful suggestions and to Sheldon Dolinger and Dennis Pandy, United Technologies Corporation, for helpful discussions.

References

1. Bruckner, A.P., "A Gun-Launched Satellite," Spaceflight, Vol. 7, 1965, pp. 118-121.
2. Eder, D., "A Low Cost Earth Based Launch System and its Effects on space Industrialization," Space Manufacturing 4; Proceedings of the 5th Conference, Princeton, NJ, May 18-21, 1981, pp. 221-229.
3. O'Neill, G.K., "The Colonization of Space," Physics Today, Vol. 27, 1974, pp. 32-40.
4. Chilton, F., Hibbs, B., Kolm, H., O'Neill, G.K., and Phillips, J., "Electromagnetic Mass Drivers," Progress in Aeronautics and Astronautics, Vol. 57, 1977, pp. 37-61.
5. Barber, J.P., "Direct Launch Using the Electric Rail Gun," Proceedings of the 1983 Jannaf Propulsion Meeting, Vol. 1, 1983, pp. 51-56.
6. Kolm, H., et al., "An Electromagnetic First Stage Space Cargo Launcher," Space Manufacturing 4; Proceedings of the 5th Conference, Princeton, NJ, May 18-21, 1981, pp. 231-233.
7. Hawke, R.S., Brooks, A.L., Fowler, C.A., and Peterson, D.R., "Electromagnetic Railgun Launchers: Direct Launch Feasibility," AIAA Journal, Vol. 20, July 1982, pp. 978-985.
8. Apel, U., "Applications and Limitations of Electromagnetic Mass-Accelerators for Future Space Transportation," Paper No. IAF-85-186, 36th Congress of the IAF, Stockholm, Sweden, October 7-12, 1985.
9. Rioux, C., Rioux-Damidau, F., Deschamps, L., "Prospects and Problems of Heavy Lift Electromagnetic Thrusters for Solar Power Satellite (SPS) Development," Paper No. IAF-85-187, 36th congress of the IAF, Stockholm, Sweden, October 7-12, 1985.
10. Winterberg, F., "The Electromagnetic Rocket Gun," Acta Astronautica, Vol. 12, 1985, pp. 155-161.
11. Miller, L.A., Rice, E.E., Earhart, R.W., and Conlon, R.J., "Preliminary Analysis of Space Mission Applications for Electromagnetic Launchers," Final Technical Report, Contract No. NAS 3-23354, Battelle Columbus Laboratories, Columbus, OH, August 30, 1984.
12. Wilbur, P.J., Mitchell, C.E. and Shaw, B.D., "The Electrothermal Ramjet," J. Spacecraft and Rockets, Vol. 20, Nov.-Dec. 1983, pp. 603-610.
13. Shaw, B.D., Mitchell, C.E. and Wilbur, P.J., "The Annular Flow, Electrothermal Plug Ramjet," J. Propulsion and Power, Vol. 1, Nov.-Dec. 1985, pp. 417-425.
14. Powers, M.V., Zaretzky, C., and Myrabo, L.N., "Analysis of Beamed Energy Ramjet/Scramjet Performance," AIAA Paper 86-1761, AIAA/SAE/ASME/ASEE 22nd Joint Propulsion Conference, Huntsville, AL, June 16-18, 1986.
15. Hertzberg, A., Bruckner, A.P. and Bogdanoff, D.W., "The Ram Accelerator: A New Chemical Method for Accelerating Projectiles to Ultrahigh Velocities," AIAA J., in press.
16. Bruckner, A.P., Bogdanoff, D.W., Knowlen, C. and Hertzberg, A., "Investigation of Gasdynamic Phenomena Associated with the Ram Accelerator Concept," AIAA Paper 87-1327, AIAA 19th Fluid Dynamics, Plasma Dynamics and Lasers Conference, Honolulu, HI, June 8-10, 1987.
17. Knowlen, C., Bruckner, A.P., Bogdanoff, D.W. and Hertzberg, A., "Performance Capabilities of the Ram Accelerator," AIAA Paper 87-2152, AIAA/SAE/ASME/ASEE 23rd Joint Propulsion Conference, San Diego, CA, June 29-July 2, 1987.
18. Bogdanoff, D.W. and Brackett, D.C., "A Computational Fluid Dynamics Code for the Investigation of Ramjet-in-Tube Concepts," AIAA Paper 87-1978, AIAA/SAE/ASME/ASEE 23rd Joint Propulsion Conference, San Diego, CA, June 29-July 2, 1987.
19. Hertzberg, A., Bruckner, A.P., Bogdanoff, D.W., and Knowlen, C., "The Ram Accelerator and its Applications: A New Chemical Approach for Reaching Ultrahigh Velocities," Proceedings of the 16th International Symposium on Shock Tubes and Waves, Aachen, West Germany, July 26-30, 1987.
20. Hertzberg, A. and Bruckner, A.P., eds., "The Ram Accelerator Concept: A Method for Direct Launch of Space Cargo to Orbit," Final Report, AA420/499, NASA/USRA Advanced Space Design Program, University of Washington, Seattle, WA, June 1987.
21. Krier, H. and Summerfield, M., eds., "Interior Ballistics of Guns: Progress in Aeronautics and Astronautics," Vol. 66, AIAA, New York, 1979.
22. Allen, H.J., Seiff, A., Winovich, W., "Aerodynamic Heating of Conical Entry Vehicles at Speeds in Excess of Earth Parabolic Speed," NASA TR R-185, 1963.

23. Allen, H.J., "The Aerodynamic Heating of Atmosphere Entry Vehicles -- A Review," in Fundamental Phenomena in Hypersonic Flow, J.F. Hall, ed., Cornell University Press, Ithaca, NY, 1966, pp. 5-29.
24. Allen, H.J. and Eggers, A.J., "A Study of the Motion and Aerodynamic Heating of Missiles Entering the Earth's Atmosphere at High Supersonic Speeds," NACA TN 4047, 1957.
25. Van Driest, E.R., "Turbulent Boundary Layer in Compressible Fluids," Journal of the Aeronautical Sciences, Vol. 18, March 1951, pp. 145-160.
26. JANAF Thermochemical Tables, 2nd ed., National Bureau of Standards, Washington, DC, 1971.
27. Ivey, H.R., Klunker, E.B. and Bowen, E.N., "A Method for Determining the Aerodynamic Characteristics of Two and Three Dimensional Shapes at Hypersonic Speeds," NACA TN 1613, 1948.
28. Voisinet, R.L.P., "Influence of Roughness and Blowing on Compressible Turbulent Boundary Layer Flow," Naval Surface Weapons Center Report No. TR-79-153, 1979.
29. Paiewansky, B.H., "Transfer Between Vehicles in Circular Orbits," Jet Propulsion, Vol. 28, 1958, pp. 212-213.

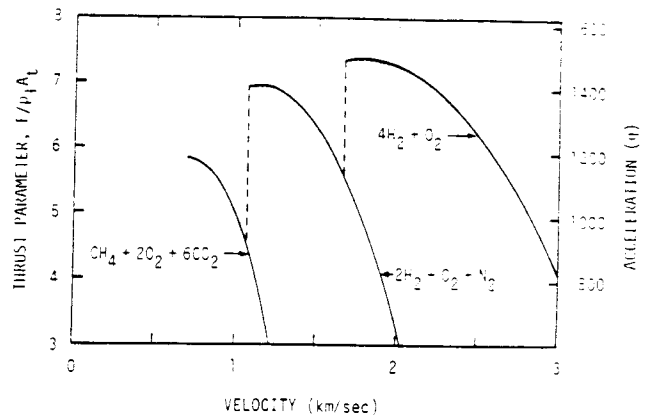


Fig. 3. Thrust parameter and acceleration as functions of velocity for subsonic thermally choked combustion ram accelerator mode. Acceleration figures are for 2000 kg 0.76 m O.D. vehicle, 1.0 m I.D. launch tube and 50 atm propellant fill pressure. Dashed lines indicate mixture transitions.

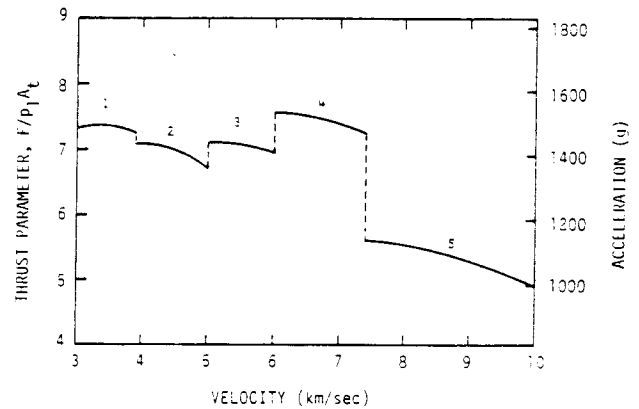


Fig. 4. Thrust parameter and acceleration as functions of velocity for superdetonative ram accelerator mode. Acceleration figures are for 2000 kg 0.76 m O.D. vehicle, 0.85 m I.D. launch tube and 50 atm propellant fill pressure. Propellant mixtures are:
 1) $2H_2 + O_2 + 2N_2 + 3Ar$
 2) $2.5H_2 + O_2 + 3.5N_2$
 3) $4.5H_2 + O_2 + 1.5N_2$
 4) $5H_2 + O_2 + 0.6N_2$
 5) $8H_2 + O_2$

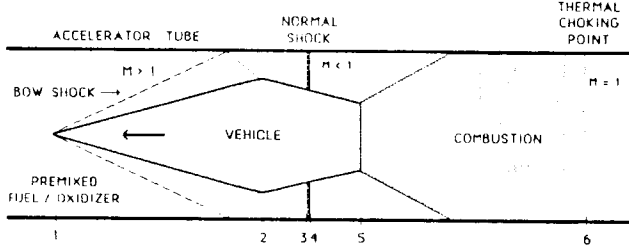


Fig. 1. Schematic of thermally choked subsonic combustion ram accelerator drive mode.

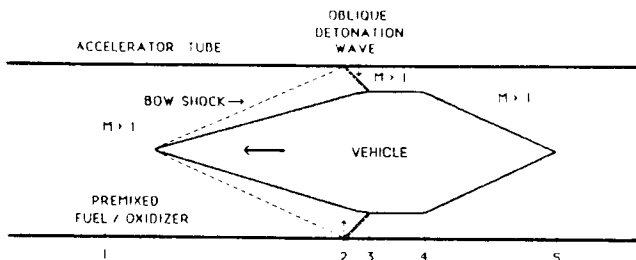


Fig. 2. Schematic of oblique detonation ram accelerator drive mode (superdetonative).

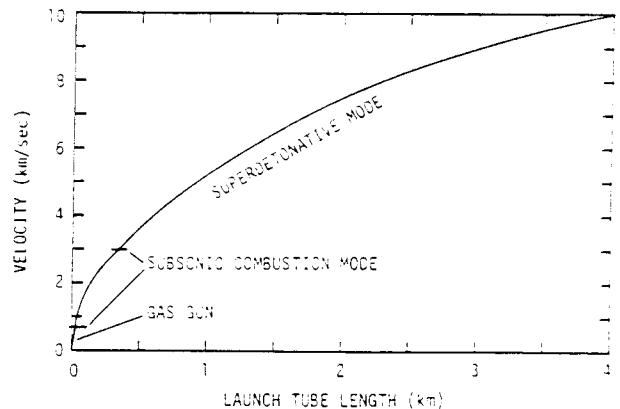


Fig. 5. Velocity profile in ram accelerator launch tube. Vehicle mass = 2000 kg.

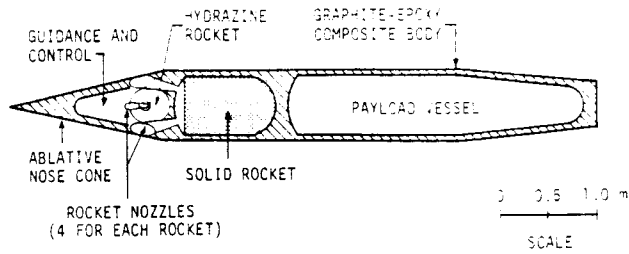


Fig. 6. Schematic of ram accelerator vehicle. Length = 6.0 m, dia = 0.76 m, nose half-angle = 12.5°.

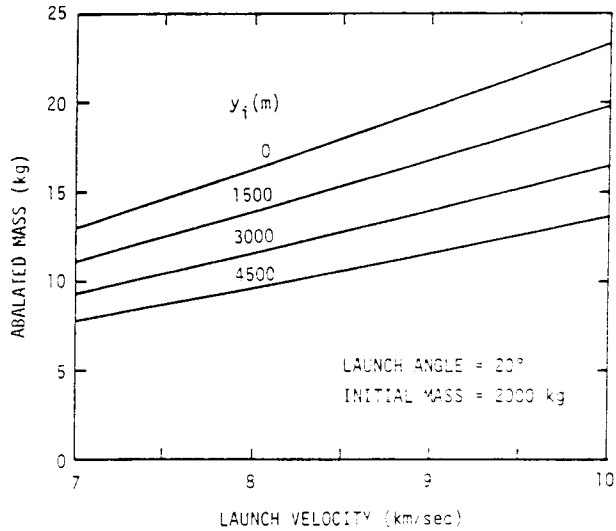


Fig. 7. Mass ablated from nose cone as a function of launch velocity and initial altitude for 20° launch angle.

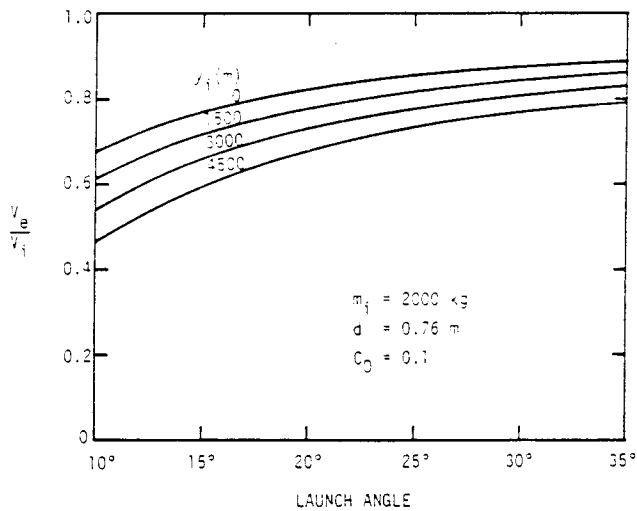


Fig. 8. Ratio of terminal velocity at "edge" of atmosphere (50 km) to initial velocity, as a function of launch angle and initial altitude. (Velocities are relative to the earth.)

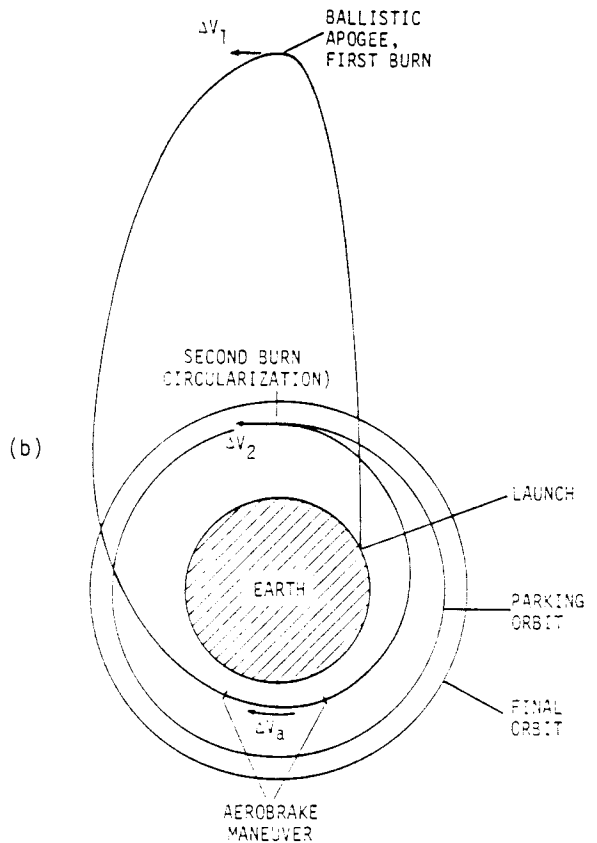
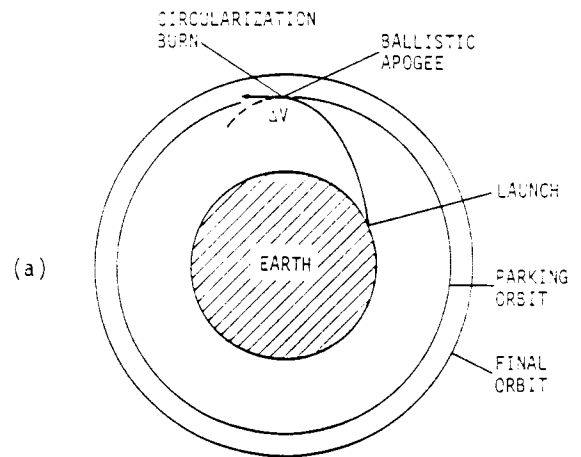


Fig. 9. Direct launch scenarios considered for ram accelerator. a) Direct insertion into parking orbit at ballistic apogee. b) Three step maneuver involving two rocket burns and aerobraking. For clarity, Hohmann transfer to final orbit is not shown.

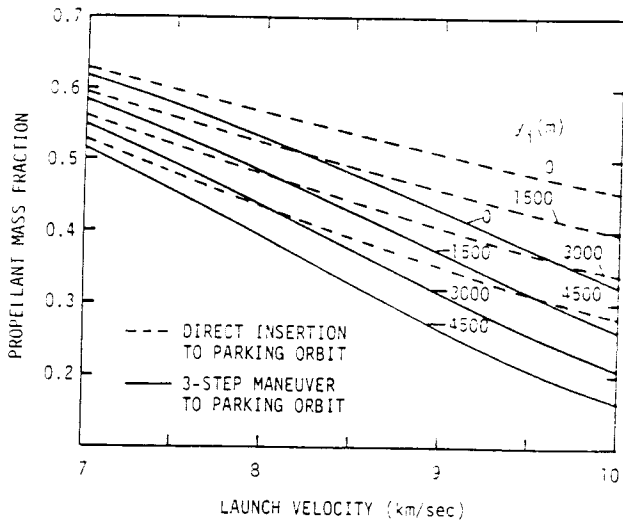


Fig. 10. Total propellant mass fraction as a function of launch velocity for circularization maneuvers shown in Figs. 9a (dashed curves) and 9b (solid curves). Parking orbit at 350 km, final orbit at 400 km. Equatorial launch. First burn uses solid rocket ($I_{sp} = 300$); all other burns use hydrazine rocket ($I_{sp} = 245$). Launch angle is optimized for each launch altitude and velocity.

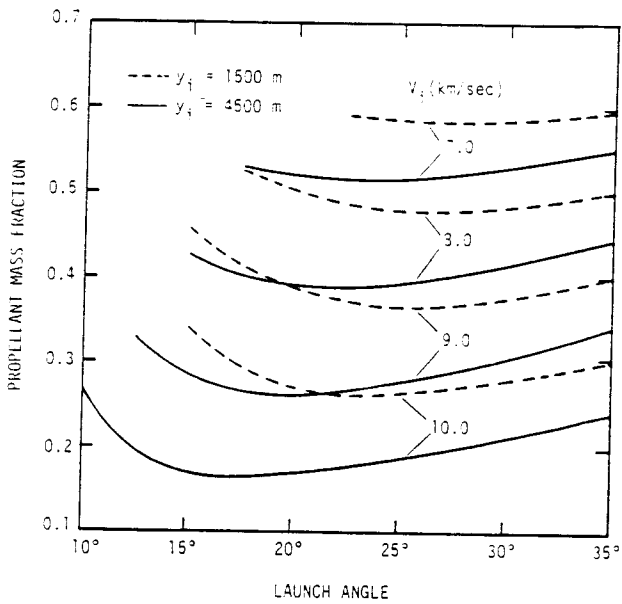


Fig. 11. Total propellant mass fraction as a function of launch angle for multi-step circularization maneuver of Fig. 9b. Parking orbit at 350 km, final orbit at 400 km. Equatorial launch. $I_{sp} = 300$ for first burn, 245 for all others.